

# Effect of Sintering Temperature on the Physical Properties of $\text{Ba}_{0.6}\text{Sr}_{0.4}\text{TiO}_3$ Prepared by Solid-State Reaction

*by* Rusiyanto Rusiyanto

---

**Submission date:** 10-Jan-2022 01:50PM (UTC+0700)

**Submission ID:** 1739437894

**File name:** 23224.pdf (1.13M)

**Word count:** 4933

**Character count:** 26307

## ORIGINAL ARTICLE

## Effect of Sintering Temperature on the Physical Properties of $\text{Ba}_{0.6}\text{Sr}_{0.4}\text{TiO}_3$ Prepared by Solid-State Reaction

Rusiyanto<sup>1</sup>, R.D. Widodo<sup>1</sup>, D.H. Al-Janani<sup>1</sup>, K. Rohmah<sup>1</sup>, J.P. Siregar<sup>2\*</sup>, A. Nugroho<sup>1</sup> and D.F. Fitriyana<sup>1</sup><sup>1</sup>Department of Mechanical Engineering, Universitas Negeri Semarang, Kampus Sekaran, Gunungpati, 50229 Semarang, Indonesia<sup>2</sup>College of Engineering, Universiti Malaysia Pahang, 26300 Gambang, Kuantan, Malaysia

**ABSTRACT** – Barium Strontium Titanate (BST) ceramic materials are widely used in electronic devices due to their stable operation at high temperatures, high tunability, low tangent loss, low DC leakage, and alterable curie temperatures. While pure BST materials are usually produced at high sintering temperatures (1250 °C), there are limited studies on the temperature and duration of the sintering process to produce pure BST, synthesised from micro or even nano-sized raw materials. This study aims to determine the effective sintering temperature for producing pure BST material using a mixture of raw materials with a mean particle size of 0.4 µm after milled for 58 hours. The  $\text{BaCO}_3$ ,  $\text{SrCO}_3$ , and  $\text{TiO}_2$  materials as raw materials for  $\text{Ba}_{0.6}\text{Sr}_{0.4}\text{TiO}_3$  synthesis were milled for 58 hours to produce a homogeneous mixture with a mean particle size of 0.4 µm. Sintering was carried out in a temperature range of 500-1100 °C for 1 hour. This study investigates the impact of sintering temperature on the physical properties and the purity of  $\text{Ba}_{0.6}\text{Sr}_{0.4}\text{TiO}_3$  powder using the x-ray diffraction method. The results showed that the  $\text{Ba}_{0.6}\text{Sr}_{0.4}\text{TiO}_3$  phase was formed at a sintering temperature of 700 °C. Pure BST material was formed at the sintering temperature of 1000 °C with a crystallite size of 41 nm. Whereas at a higher sintering temperature (1100 °C), the pure BST material formed produced a larger crystallite, sized at 43 nm with cubic structure. The synthesis temperature and duration recorded in this research are lower than recorded in the BST material preparation using the solid-state method. The results of this study indicate that the sintering temperature greatly affects the purity, crystal system and crystallite size of the  $\text{Ba}_{0.6}\text{Sr}_{0.4}\text{TiO}_3$  material produced. The sintering temperature of 1100 °C produces  $\text{Ba}_{0.6}\text{Sr}_{0.4}\text{TiO}_3$  material with the best physical properties because it has a cubic-shaped crystal system and the largest crystal size.

**ARTICLE HISTORY**Received: 18<sup>th</sup> Aug 2020Revised: 22<sup>nd</sup> Mar 2021Accepted: 11<sup>th</sup> June 2021**KEYWORDS**

Particle-size;

Crystallite-size

Barium-strontium titanate;

Solid-state reaction

**INTRODUCTION**

Barium Strontium Titanate (BST),  $\text{Ba}_x\text{Sr}_{(1-x)}\text{TiO}_3$ ,  $0 < x < 1$ , is a ferroelectric material with a perovskite structure. This material composes of barium titanate ( $\text{BaTiO}_3$ ) and strontium titanate ( $\text{SrTiO}_3$ ). When  $\text{SrTiO}_3$  is added to  $\text{BaTiO}_3$ , Sr ion replaces Ba ion to form the BST material structure. Barium strontium titanate ceramic material is widely used in electronic devices [1]. As bulk ceramics and thin films, this material has a unique combination of large dielectric constant. It demonstrates a stable operation at high temperature, high tunability, low loss tangent, low DC leakage, and alterable curie temperature [2]. The uniqueness of the BST material is attributed to several factors, such as the Ba / Sr ratio, the synthesis method, and the particle and crystal size [3].  $\text{Ba}_x\text{Sr}_{(1-x)}\text{TiO}_3$  ceramics with various compositions of x (Ba / Sr ratio) has been widely studied; for example  $x = 0.2, 0.3, 0.4, 0.5$ , and  $0.6$  [4]. X-ray diffraction (XRD) results showed BST crystals formation in all variations of x; after the sintering process was carried out at 1000 °C for 3 hours. However, there was still a secondary phase ( $\text{Sr}_2\text{TiO}_4$ ,  $\text{SrTiO}_{10}$ , and  $\text{Sr}_3\text{Ti}_2\text{O}_7$ ). This can be improved by increasing the sintering temperature. The secondary phase can be removed by increasing the sintering temperature. Increasing the concentration of x causes a transformation of the crystal system from tetragonal to cubic. The grain size and density of the sample decrease with increasing concentration x because Sr is having a smaller radius than Ba. Curie temperatures for samples with  $x = 0.2, 0.3, 0.4, 0.5$ , and  $0.6$  were 70 °C, 28.7 °C, -8.4 °C, -45.5 °C, and -82.6 °C, respectively. Curie temperature decreased with increasing x concentration. The highest dielectric constant found in sample with  $x = 0.3$  [4]. Furthermore, the high dielectric and pyroelectric properties of the composition  $\text{Ba}_x\text{Sr}_{(1-x)}\text{TiO}_3$  with  $0.3 \leq x \leq 0.5$  resulted in the Curie temperature (TC) or ferroelectric-paraelectric phase transformation temperature decrease, near to room temperature (25 °C) [5].

$\text{Ba}_x\text{Sr}_{(1-x)}\text{TiO}_3$  materials are generally synthesised by hydrothermal method, sol-gel method, and conventional solid-state reaction method [6]. The BST material synthesised by the hydrothermal and sol-gel method produces crystals less than 100 nm. Subsequently, it produces residual hydroxide ions, which resulted in the formation of intergranular pores [7]. The mechanochemical or solid-state method is the most used method for BST nanoparticles large-scale production [8]. The solid-state method has several advantages; it uses low-cost raw materials, simple synthesis processes, and the ability to produce fine particles [8]. During solid-state processes such as high-energy ball milling, the steps that occur during solid-state processes, specifically welding, deformation, and fracture of powder raw materials, are repeated [9].

\*CORRESPONDING AUTHOR | J.P. Siregar | [januar@ump.edu.my](mailto:januar@ump.edu.my)

The mechanical activation during solid-state reaction with mechanical milling increases the raw material specific surface area due to the destruction of agglomerates and particles of the initial precursors [10]. In this regard, the mechanical milling process can produce particles sized  $> 1 \mu\text{m}$ . In general, the microstructure of the particle and crystallite size of mechanical milling products were influenced by the characteristics of the raw materials used, duration and heating temperature during the mechanical milling process [11].

In recent years, several studies have focused on the effect of sintering temperature on the synthesis of Barium Strontium Titanate (BST). In general, the increase of the temperature and duration time of the sintering process affected the BST material's purity and increased the crystallite size [12]. Pure BST materials are usually produced at high sintering temperatures [4], [12]–[18]. Sandi et al. carried out a sintering process at  $1200^\circ\text{C}$  for 2 hours to produce pure BST material by the solid-state reaction method [8]. Yustanti et al. reported that the sintering raw materials measuring an average size of  $2.4 \mu\text{m}$  at a temperature of  $1200^\circ\text{C}$  produced pure BST material without the presence of impurities [14]. In the meantime, barium strontium titanate ceramic material was synthesised from fine constituent powders produced from high energy ball milling processes at sintering temperatures  $1200\text{--}1350^\circ\text{C}$ , as reported by Mudinepalli et al. [12]. Budkhod et al. performed sintering at temperatures between  $1050\text{--}1350^\circ\text{C}$  to produce  $\text{Ba}_{0.7}\text{Sr}_{0.3}\text{TiO}_3$  ceramics using a hybrid method between solid-state reaction and sol-gel combustion methods using urea as a fuel [15]. Meanwhile, Gate et al. conducted a sintering process at a temperature of  $1100^\circ\text{C}$  for 3 hours to produce a pure  $\text{Ba}_{0.6}\text{Sr}_{0.4}\text{TiO}_3$  material using the sol-gel method [17]. Lastly, Zhu et al. synthesised barium strontium titanate glass and ceramics using the sol-gel method and was sintered at temperatures between  $1000$  and  $1150^\circ\text{C}$  [18].

The high sintering temperature to produce pure BST material has prompted various studies to produce pure BST materials at lower sintering temperatures using glass, polymer and inorganic additives [19]. One way to produce BST material at low sintering temperatures is to add  $\text{Li}_2\text{O}$  material, as reported by Zhang et al. [20]. Zhang et al. investigated the effect of adding  $\text{Li}_2\text{O}$  on the sintering temperature of commercial BST. It was found that by adding  $0.5 \text{ wt}\%$ ,  $\text{Li}_2\text{O}$  could reduce the sintering temperature to  $900^\circ\text{C}$  without decreasing the ceramics performance. The sintering temperature of BST materials was reduced from  $1350^\circ\text{C}$  to  $900^\circ\text{C}$  by adding Li [21]. However, the XRD test showed two secondary phases as impurities caused by the addition of lithium. Besides, this research method has many limitations when applied to commercial production because it requires a very high cost [19], [21].

However, the BST material sintering ability decreased along with the broader particle size distribution [22]. Accordingly, reducing the particle size is another way that can be used to speed up or shorten the sintering time. The sintering temperature is reduced with smaller raw material particles. The smaller the raw material particle size, the faster the grain becomes coarse due to the high particle surface energy compared to the large grain size distribution in the batch under the same sintering conditions [23]. In another reference, the raw material with smaller dimensions causes a larger contact surface so that the sinterability increases due to the maximal diffusion process [24]. Therefore, this study uses a vibratory ball milling for 58 hours to mix  $\text{BaCO}_3$ ,  $\text{SrCO}_3$ , and  $\text{TiO}_2$  to obtain a homogeneous mixture with a mean particle size of  $0.4 \mu\text{m}$ . This research aims to determine the effective sintering temperature to produce pure BST material using a mixture of  $\text{BaCO}_3$ ,  $\text{SrCO}_3$ , and  $\text{TiO}_2$  ball-milled for 58 hours.

## METHODS AND MATERIALS

$\text{Ba}_{0.6}\text{Sr}_{0.4}\text{TiO}_3$  was synthesised from  $\text{BaCO}_3$ ,  $\text{SrCO}_3$ , and  $\text{TiO}_2$  powders using the mechanical alloying method with a purity level of 99%. The powders were obtained from Sigma-Aldrich. The particle size analyser (PSA) test results in Table 1 show the  $\text{BaCO}_3$ ,  $\text{SrCO}_3$ , and  $\text{TiO}_2$  powders average sizes. Meanwhile, the results of XRD tests on  $\text{TiO}_2$ ,  $\text{SrCO}_3$ , and  $\text{BaCO}_3$  powders are shown in Figure 1(a). The diffraction patterns of  $\text{TiO}_2$ ,  $\text{SrCO}_3$  and  $\text{BaCO}_3$  powders are in line with the diffraction patterns of  $\text{TiO}_2$ ,  $\text{SrCO}_3$  and  $\text{BaCO}_3$  in the Inorganic Crystal Structure Database (ICSD), respectively, with numbers 98-009-6946, 98-016-6088, and 98-016-6090. The Rietveld analysis using High Score Plus software shows that the  $\text{TiO}_2$  powder has tetragonal-shaped crystal systems while the  $\text{SrCO}_3$  and  $\text{BaCO}_3$  powders have orthorhombic crystal systems.

**Table 1.** Average particle size of  $\text{BaCO}_3$ ,  $\text{SrCO}_3$  and  $\text{TiO}_2$ .

Raw materials	Average particle size ( $\mu\text{m}$ )
$\text{BaCO}_3$	1.979
$\text{SrCO}_3$	3.182
$\text{TiO}_2$	0.795

In this research,  $\text{BaCO}_3$ ,  $\text{SrCO}_3$  and  $\text{TiO}_2$  powders were subjected to a wet milling process using a vibratory ball milling machine with a composition of 41.63 grams each, 20.76 grams, and 28.08 grams for 58 hours. The ball to powder ratio (BPR) in the milling process is 10:1. After 58 hours, the mixed  $\text{BaCO}_3$ ,  $\text{SrCO}_3$  and  $\text{TiO}_2$  were tested for PSA and XRD. The PSA test results showed that the powder mixture of  $\text{BaCO}_3$ ,  $\text{SrCO}_3$  and  $\text{TiO}_2$  had a particle size of  $0.4 \mu\text{m}$ . Meanwhile, according to the Rietveld analysis using the High Score Plus software, the XRD test results are shown in Figure 1(b). Figure 1(b) shows no change in the diffraction pattern of the powder of  $\text{TiO}_2$ ,  $\text{SrCO}_3$  and  $\text{BaCO}_3$ . The crystal sizes of  $\text{BaCO}_3$ ,  $\text{SrCO}_3$  and  $\text{TiO}_2$  calculated using The Williamson-Hall method are 48 nm, 61 nm, and 71 nm, respectively.

After characterising the mixture of milled  $\text{TiO}_2$ ,  $\text{SrCO}_3$ , and  $\text{BaCO}_3$  powders, the next step is sintering the powder mixture of  $\text{TiO}_2$ ,  $\text{SrCO}_3$  and  $\text{BaCO}_3$ . The sintering process was carried out in the electric chamber furnace (Nabertherm

N31/H) with temperature variations of 500 °C, 600 °C, 700 °C, 800 °C, 900 °C, 1000 °C, and 1100 °C in the air under atmospheric pressure up to 1 hour. After the sintering process, characterisation was carried out using the XRD methods. The Philips XRD was also used to analyse the resulting phase and crystallite size. The step-scan method was performed to record the x-ray diffraction patterns. The intensity data during the scanning was taken every 2 seconds for each step on the diffraction angle of 0.005°. The Rietveld analysis was conducted using the High Score Plus software. The description of the diffraction line profiles at Rietveld refinement was achieved using the pseudo-Voigt function.

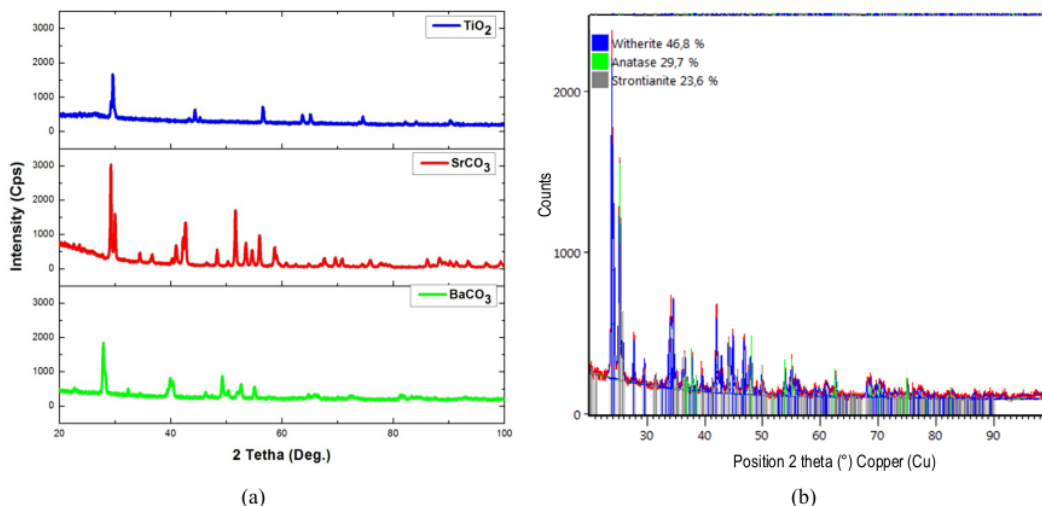


**Figure 1.** X-ray diffraction patterns of  $\text{TiO}_2$ ,  $\text{SrCO}_3$  and  $\text{BaCO}_3$  powders (a) before and (b) after 58 hours of milling.

## RESULTS AND DISCUSSION

Figure 2 shows the diffraction pattern of  $\text{BaCO}_3$ ,  $\text{SrCO}_3$ , and  $\text{TiO}_2$  powder mixture at each sintering temperature. From the figure, the  $\text{Ba}_{0.6}\text{Sr}_{0.4}\text{TiO}_3$  phase was not formed in the material sintered at temperatures of 500 °C and 600 °C. Meanwhile, while the  $\text{Ba}_{0.6}\text{Sr}_{0.4}\text{TiO}_3$  phase was formed at temperatures of 700 °C, 800 °C and 900 °C, other compound phases,  $\text{BaCO}_3$ ,  $\text{SrCO}_3$ ,  $\text{TiO}_2$  and  $\text{BaTiO}_3$ , were observed. Moreover, a single-phase  $\text{Ba}_{0.6}\text{Sr}_{0.4}\text{TiO}_3$  was formed at temperatures of 1000 °C and 1100 °C.

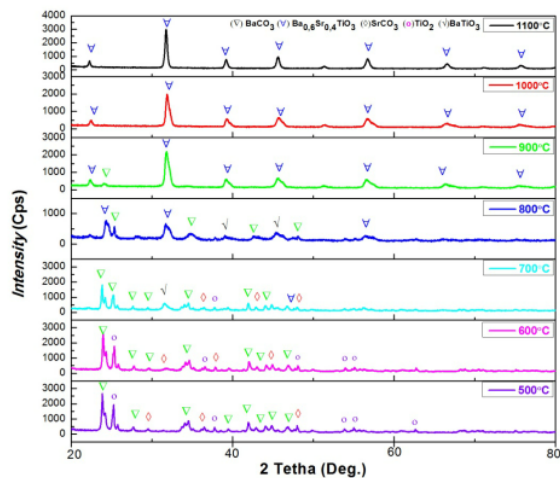


**Figure 2.** X-ray diffraction patterns of the sintered samples.

Figure 3 shows the Rietveld analysis results using the High Score Plus software based on X-ray diffraction obtained from the test results. Figure 3(a) shows the x-ray diffraction pattern on a powder that has been sintered at 500 °C. The x-ray diffraction pattern shows that the  $\text{Ba}_{0.6}\text{Sr}_{0.4}\text{TiO}_3$  phase was not formed. In this light, the phases formed at 500 °C sintering temperature variations are  $\text{BaCO}_3$  (withierite),  $\text{TiO}_2$  (anatase), and  $\text{SrCO}_3$  (strontianite), with the respective percentage of 48.3%; 27.2%, and 24.5%. Meanwhile, the crystallite size formed in  $\text{BaCO}_3$ ,  $\text{TiO}_2$ , and  $\text{SrCO}_3$  was 54.7 nm, 125.6 nm, and 80.3 nm. The x-ray diffraction pattern of the sintered powder at 600 °C is shown in Figure 3(b). At

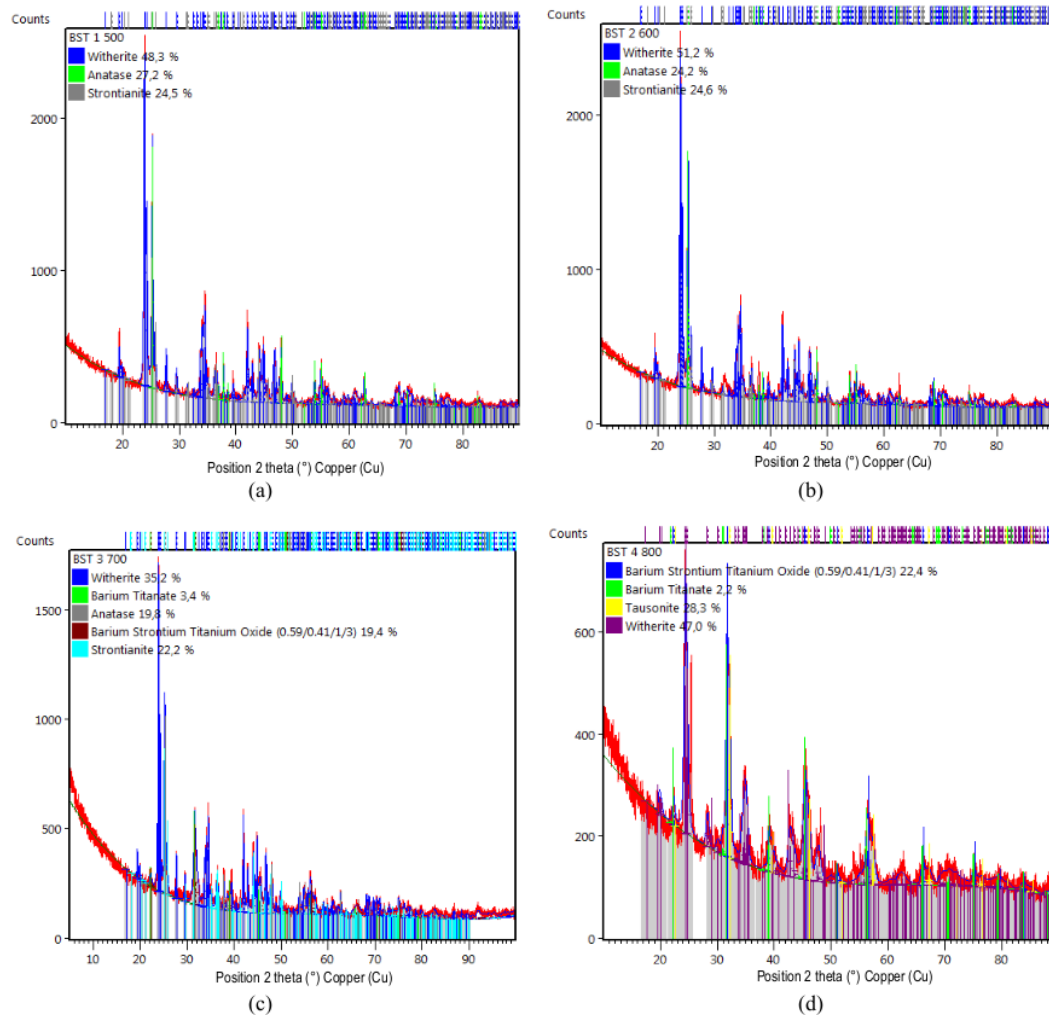


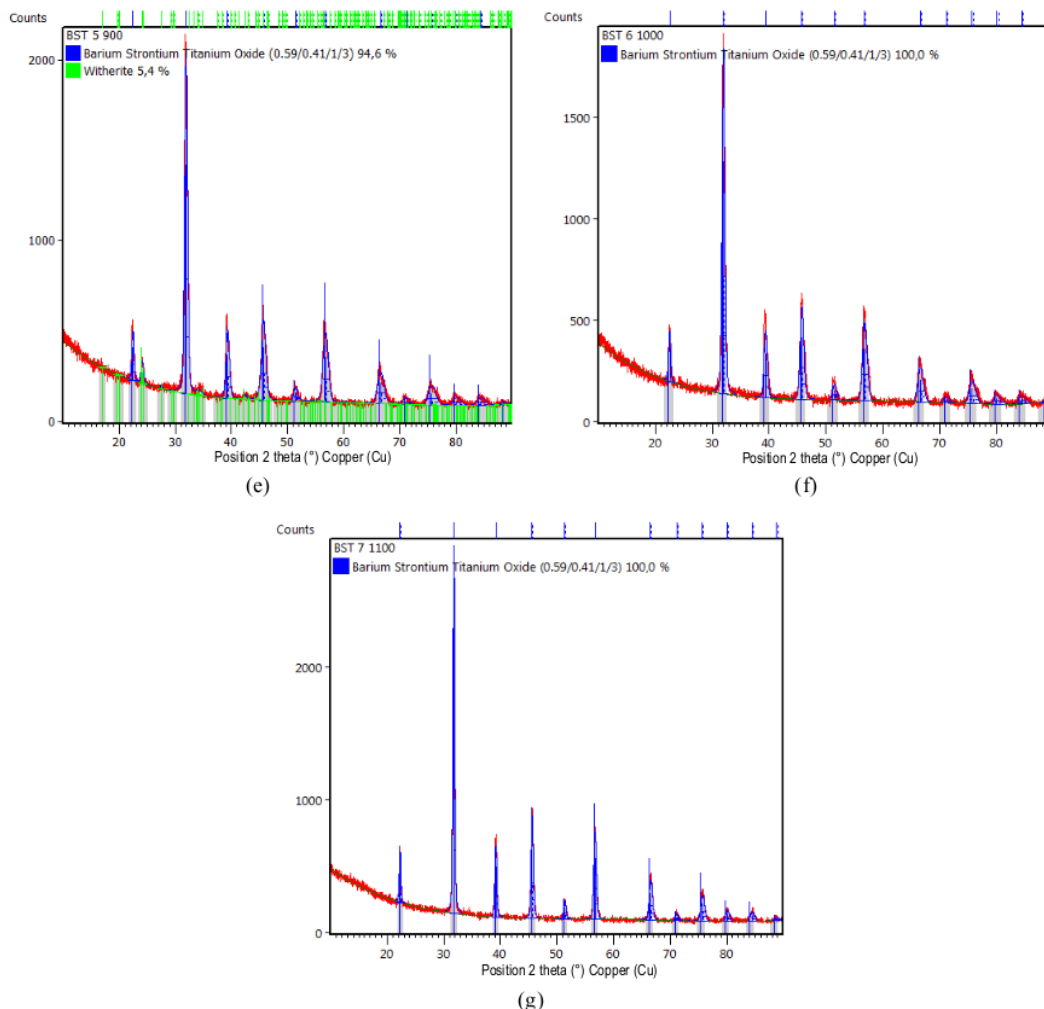
600 °C,  $Ba_{0.6}Sr_{0.4}TiO_3$  was not formed and still in the  $BaCO_3$ ,  $TiO_2$ , and  $SrCO_3$  phases, with 51.2%; 24.2% and 24.6%, respectively. The sizes of the crystallites formed after sintering  $BaCO_3$ ,  $TiO_2$ , and  $SrCO_3$  at 600 °C for are 56.4 nm, 104.3 nm, and 122.3 nm, respectively.

Figure 3(c) shows the x-ray diffraction pattern of a mixture of  $BaCO_3$ ,  $SrCO_3$ , and  $TiO_2$  powders sintered at 700 °C. At a temperature of 700 °C, the  $Ba_{0.6}Sr_{0.4}TiO_3$  phase was formed with a percentage of 19.4% and a crystallite size of 15.3 nm. However, at 700 °C, the  $BaCO_3$ ,  $SrCO_3$  and  $TiO_2$  phases were still found at a respective percentage of 35.2%, 22.2%, and 19.8%, and crystallite sizes of 58.1 nm; 65.6 nm and 66.2 nm, respectively. Apart from  $Ba_{0.6}Sr_{0.4}TiO_3$ ,  $BaCO_3$ ,  $SrCO_3$  and  $TiO_2$  phases, a new phase,  $BaTiO_3$  at 3.4% and crystallite size of 38 nm, was also formed.

Figure 3(d) shows that the crystallite percentage increased to 22.4%, and its size increased to 30.3 nm at the  $Ba_{0.6}Sr_{0.4}TiO_3$  phase when sintering at 800 °C. In this variation, the crystal size of  $Ba_{0.6}Sr_{0.4}TiO_3$  is two times the crystallite size formed at 700 °C sintering temperature. Meanwhile, the  $BaTiO_3$  phase percentage decreased to 2.2%, accompanied by a decrease in crystal size to 19.5 nm.  $BaCO_3$  phases were still found with a composition of 47% with a crystallite size of 40 nm. Apart from  $Ba_{0.6}Sr_{0.4}TiO_3$ ,  $BaCO_3$ , and  $BaTiO_3$  phases, a new phase,  $SrTiO_3$  was also formed at 28.3% and crystallite size of 32.6 nm.

Figure 3(e) shows the x-ray diffraction pattern at a product sintering temperature of 900 °C. The  $Ba_{0.6}Sr_{0.4}TiO_3$  phase formed in this variation experienced a significant increase with a percentage of 94.6% and a crystallite size of 40.1 nm. Simultaneously, the other 5.4% is the  $BaCO_3$  phase with a crystallite size of 21.5 nm. The single phase of  $Ba_{0.6}Sr_{0.4}TiO_3$  was formed perfectly at various sintering temperatures of 1000 °C and 1100 °C, as shown in Figure 3(f) and 3(g).  $Ba_{0.6}Sr_{0.4}TiO_3$  with crystallites size of 30 nm and 43 nm resulted in sintering temperatures of 1000 °C and 1100 °C.





**Figure 3.** X-ray diffraction patterns of sintered samples at (a) 500 °C, (b) 600 °C, (c) 700 °C (d) 800 °C, (e) 900 °C, (f) 1000 °C and (g) 1100 °C.

The results of this study indicate that the  $\text{Ba}_{0.6}\text{Sr}_{0.4}\text{TiO}_3$  material has begun to form at a sintering temperature of 700 °C. However, a secondary phase is still formed and completely into single-phase  $\text{Ba}_{0.6}\text{Sr}_{0.4}\text{TiO}_3$  at 1000°C and 1100°C. The effect of sintering temperature on the phase composition (%) and crystallite sizes of  $\text{Ba}_{0.6}\text{Sr}_{0.4}\text{TiO}_3$  formed is shown in Figure 4. The impurity phase disappears proportionately with the increase in sintering temperature. The kinetic energy in atoms increases due to higher sintering temperatures. The higher temperature makes it easier for the atoms to interact and bond with each other, causing the impurity phase to disappear [12], [17]. Besides, increasing the sintering temperature causes the atomic bonds to become stronger. Thus, sintering carried out at 1000°C and 1100°C resulted in forming a single phase of  $\text{Ba}_{0.6}\text{Sr}_{0.4}\text{TiO}_3$  which is more stable. Increasing the sintering temperature will result in a recrystallisation process in the raw materials ( $\text{BaCO}_3$ ,  $\text{SrCO}_3$ , and  $\text{TiO}_2$ ) so that a more stable  $\text{Ba}_{0.6}\text{Sr}_{0.4}\text{TiO}_3$  phase is formed. An increase in sintering temperature will produce  $\text{Ba}_{0.6}\text{Sr}_{0.4}\text{TiO}_3$  with a higher phase composition (%). The crystallite sizes also increased, as reported in previous studies [12], [17], [25], [26].

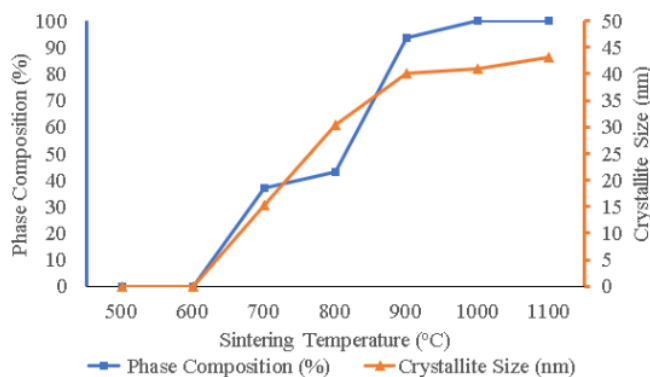


**Figure 4.** The effect of sintering temperature on the physical properties of  $\text{Ba}_{0.6}\text{Sr}_{0.4}\text{TiO}_3$ .

The use of  $\text{BaCO}_3$ ,  $\text{SrCO}_3$ , and  $\text{TiO}_2$  powder mixture, with a particle size of  $0.4 \mu\text{m}$ , has been proven to produce  $\text{Ba}_{0.6}\text{Sr}_{0.4}\text{TiO}_3$  material at lower sintering temperatures with a faster duration (1 hour). This is supported by [27] and [24] study, which revealed that reducing the particle size of raw materials is another method that can be used to speed up sintering and shorten sintering time. The sintering temperature is reduced with smaller raw material particles. The smaller the raw material particle size, the faster the grain becomes coarse due to the high particle surface energy compared to the large grain size distribution in the batch under the same sintering conditions [27]. Previous research [24] mentioned raw materials with smaller dimensions causes a larger contact surface so that the sinterability increases due to the maximum diffusion process. In this study, sintering carried out at temperatures of  $1000^\circ\text{C}$  and  $1100^\circ\text{C}$  for 1 hour produced single-phase  $\text{Ba}_{0.6}\text{Sr}_{0.4}\text{TiO}_3$ . In this study, single-phase  $\text{Ba}_{0.6}\text{Sr}_{0.4}\text{TiO}_3$  resulted in lower sintering temperature and shorter sintering duration compared to the results of the study conducted by [4], [12], [14], [17], [26]. These studies' results showed the single-phase formation of  $\text{Ba}_{0.6}\text{Sr}_{0.4}\text{TiO}_3$  was carried out in a sintering temperature range of  $1100^\circ\text{C}$ – $1350^\circ\text{C}$  with a sintering duration of  $\geq 2$  hours.

In addition, [4], [12], [14], [26], [28] have clearly shown that the decrease in calcination or sintering temperature is due to the reduction in the small particle size of the raw materials; ranging from submicrometer or even to the nanoscale. The use of a smaller particle size increases the contact area and decreases the reactants contact distance, thereby increasing the overall reaction kinetics. The results of this study indicate that the sintering temperature greatly affects the purity, crystal system, and crystallite size of the material  $\text{Ba}_{0.6}\text{Sr}_{0.4}\text{TiO}_3$  produced. The effect of sintering temperature on the physical properties of  $\text{Ba}_{0.6}\text{Sr}_{0.4}\text{TiO}_3$  formed is shown in Table 2. The higher the sintering temperature resulted in a sharper peak intensity at  $\text{Ba}_{0.6}\text{Sr}_{0.4}\text{TiO}_3$ , which indicates an increase in crystal size. Accordingly, the higher the sintering temperature used, the higher the crystal size of the material  $\text{Ba}_{0.6}\text{Sr}_{0.4}\text{TiO}_3$  formed. This is supported by the studies of [4], [17], [26], [29]. Thus, increasing the sintering temperature increased the atoms kinetic energy to diffuse and make the atoms react and bond perfectly. This finding is supported by other studies [29]–[32] that found that the crystallites produced have a larger size and higher crystallinity.

**Table 2.** The Physical Properties in The Formation of  $(\text{Ba}_{0.6}\text{Sr}_{0.4})\text{TiO}_3$ .

Sintering temperature ( $^\circ\text{C}$ )	Phase	Composition phase (%)	Crystal system	Crystallite size (nm)
500	$\text{BaCO}_3$	48	Orthorhombic	54.7
	$\text{TiO}_2$	27	Tertragonal	125.6
	$\text{SrCO}_3$	25	Orthorhombic	80.3
600	$\text{BaCO}_3$	51.2	Orthorhombic	56.4
	$\text{TiO}_2$	24.2	Tertragonal	104.3
	$\text{SrCO}_3$	24.6	Orthorhombic	122.3
700	$\text{BaCO}_3$	35.2	Orthorhombic	58.1
	$\text{TiO}_2$	19.8	Tertragonal	19.8
	$\text{SrCO}_3$	22.2	Orthorhombic	65.6
	$\text{BaTiO}_3$	3.4	Orthorhombic	38
	$(\text{Ba}_{0.67}\text{Sr}_{0.33})\text{TiO}_3$	19.4	Tertragonal	15.3
800	$\text{BaCO}_3$	47	Orthorhombic	40
	$\text{BaTiO}_3$	2.2	Orthorhombic	19.5
	$\text{SrTiO}_3$	28.3	Orthorhombic	32.6
	$(\text{Ba}_{0.67}\text{Sr}_{0.33})\text{TiO}_3$	22.4	Tertragonal	30.3
900	$\text{BaCO}_3$	5.4	Orthorhombic	21.5
	$(\text{Ba}_{0.67}\text{Sr}_{0.33})\text{TiO}_3$	94.6	Tertragonal	40.1
1000	$(\text{Ba}_{0.59}\text{Sr}_{0.41})\text{TiO}_3$	100	Cubic	41
1100	$(\text{Ba}_{0.6}\text{Sr}_{0.4})\text{TiO}_3$	100	Cubic	43

In addition, an increase in the sintering temperature in this study caused changes in the crystal system of the  $\text{Ba}_{0.6}\text{Sr}_{0.4}\text{TiO}_3$  material. At temperatures of 700 °C, 800 °C, and 900 °C, the crystal system in the material  $\text{Ba}_{0.6}\text{Sr}_{0.4}\text{TiO}_3$  is tetragonal. Whereas at temperatures of 1000 °C and 1100 °C, the crystal system in the  $\text{Ba}_{0.6}\text{Sr}_{0.4}\text{TiO}_3$  is cubic with a higher peak intensity with increasing sintering temperature. The  $\text{Ba}_{0.6}\text{Sr}_{0.4}\text{TiO}_3$  with cubic structure increased the dielectric properties of the material  $\text{Ba}_{0.6}\text{Sr}_{0.4}\text{TiO}_3$  produced [12], [17], [33]. Besides the crystal structure, the dielectric properties of the  $\text{Ba}_{0.6}\text{Sr}_{0.4}\text{TiO}_3$  material are also influenced by the crystal size, where the dielectric property increases with the crystallite size [12], [29], [34]. In this study, the sintering temperature of 1100 °C produces  $\text{Ba}_{0.6}\text{Sr}_{0.4}\text{TiO}_3$  material with the best physical properties because it has a cubic-shaped crystal system and the largest crystal size.

## CONCLUSION

The effect of sintering temperature on the physical properties of  $\text{Ba}_{0.6}\text{Sr}_{0.4}\text{TiO}_3$  material synthesised with 0.4 µm raw materials (and milled up to 58 hour) using the solid-state reaction method has been investigated. The use of raw materials, a mixture of  $\text{BaCO}_3$ ,  $\text{SrCO}_3$ , and  $\text{TiO}_2$  with a particle size of 0.4 µm could produce  $\text{Ba}_{0.6}\text{Sr}_{0.4}\text{TiO}_3$  material at a lower sintering temperature of 700 °C. Moreover, the single-phase  $\text{Ba}_{0.6}\text{Sr}_{0.4}\text{TiO}_3$  can be produced at temperatures of 1000 °C and 1100 °C. Increasing the sintering temperature in this study resulted in  $\text{Ba}_{0.6}\text{Sr}_{0.4}\text{TiO}_3$  material with higher purity as marked by the disappearance of the  $\text{BaTiO}_3$ ,  $\text{BaCO}_3$ ,  $\text{SrCO}_3$ , and  $\text{TiO}_2$  phases. Higher sintering temperature increased the crystal size and changed the crystal system from tetragonal to cubic. The sintering temperature of 1100 °C produces  $\text{Ba}_{0.6}\text{Sr}_{0.4}\text{TiO}_3$  material with the best physical properties because it has a cubic-shaped crystal system and the largest crystal size.

## ACKNOWLEDGEMENT

We would like to express our gratitude to the Ministry of Research and Higher Education for funding this research through Competitive Research Grant with No. 042.06.1.401516/2016.

## REFERENCES

- [1] Szafraniak B, Fušnik L, Xu J, et al. Semiconducting metal oxides:  $\text{SrTiO}_3$ ,  $\text{BaTiO}_3$  and  $\text{BaSrTiO}_3$  in gas-sensing applications: A review. *Coatings* 2021; 11: 1–23.
- [2] Sangle AL, Lee OJ, Kursumovic A, et al. Very high commutation quality factor and dielectric tunability in nanocomposite  $\text{SrTiO}_3$  thin films with  $T_c$  enhanced to >300 °C. *Nanoscale* 2018; 10: 3460–3468.
- [3] Vigneshwaran B, Kuppasami P, Ajithkumar S, et al. Study of low temperature-dependent structural, dielectric, and ferroelectric properties of  $\text{Ba}_x\text{Sr}_{1-x}\text{TiO}_3$  ( $x = 0.5, 0.6, 0.7$ ) ceramics. *Journal of Materials Science: Materials in Electronics* 2020; 31: 10446–10459.
- [4] Gatea HA, Naji IS. The effect of Ba/Sr ratio on the Curie temperature for ferroelectric barium strontium titanate ceramics. *Journal of Advanced Dielectrics* 2020; 10: 1–11.
- [5] Vu T-H, Phuong NTM, Nguyen T. Lead-free ferroelectric barium titanate -based thin film for tunable microwave device application. *IOP Conference Series: Materials Science and Engineering* 2021; 1091: 012060.
- [6] Alwan H, Jasim S. Preparation and characterization of  $\text{Ba}_{1-x}\text{Sr}_x\text{TiO}_3$  by sol-gel method. *Asian Journal of Chemistry* 2019; 31: 186–190.
- [7] Panomsuwan G, Manuspiya H. Morphological and structural properties of barium strontium titanate nanopowders synthesized via a sol-gel method. *Ferroelectrics* 2020; 554: 30–37.
- [8] Sandi DK, Supriyanto A, Jamaluddin A, et al. The influences of mole composition of strontium (x) on properties of barium strontium titanate ( $\text{Ba}_{1-x}\text{Sr}_x\text{TiO}_3$ ) prepared by solid state reaction method. *AIP Conference Proceedings* 2016; 1710: 1–5.
- [9] Dulkan P. Solid-state mechanochemical syntheses of perovskites. In: Pan L, Zhu G, editors. *Perovskite Materials - Synthesis, Characterisation, Properties, and Applications*. London: InTech-Open, 2016, p 3–26.
- [10] Zhang L, Huang Z, Liu Y, et al. Effects of mechanical ball milling time on the microstructure and mechanical properties of  $\text{Mo}(2)\text{NiB}(2)\text{-Ni}$  Cermets. *Materials* 2019; 12(12), 1926.
- [11] Widodo RD, Manaf A. Physical characteristics and magnetic properties of  $\text{BaFe}_{12}\text{O}_{19}/\text{SrTiO}_3$  based composites derived from mechanical alloying. *AIP Conference Proceedings* 2016; 1725: 125–132.
- [12] Mudinepalli VR, Feng L, Lin WC, et al. Effect of grain size on dielectric and ferroelectric properties of nanostructured  $\text{Ba}_{0.8}\text{Sr}_{0.2}\text{TiO}_3$  ceramics. *Journal of Advanced Ceramics* 2015; 4: 46–53.
- [13] Elqudsy MA, Widodo RD, Rusiyanto, et al. The particle and crystallite size analysis of  $\text{BaTiO}_3$  produced by conventional solid-state reaction process. *AIP Conference Proceedings* 2017; 1818: 020012.
- [14] Yustanti E, Hafizah M, Manaf A. The effect of milling time and sintering temperature on formation of nanoparticles barium strontium titanate. *AIP Conference Proceedings* 2017; 1788: 30099.
- [15] P Budkhod NS and ST. Synthesis of  $\text{Ba}_{0.7}\text{Sr}_{0.3}\text{TiO}_3$  ceramics via hybrid method. *Journal of Physics: Conference Series* 2018; 252: 0–5.
- [16] Trobough ND. Examination of Dielectric Properties of  $\text{BaTiO}_3$ - $\text{SrTiO}_3$  Based Systems. BSc Thesis, Oregon State University, USA, 2020.
- [17] Gatea HA, Naji IS. Impact of sintering temperature on structural and dielectric properties of barium strontium titanate prepared



- by sol-gel method. *Journal of Ovonic Research* 2018; 14: 467–474.
- [18] Zhu J, Zhang Y, Song X, et al. Influence of sintering temperature on microstructures and energy-storage properties of barium strontium titanate glass-ceramics prepared by sol-gel process. *Physica Status Solidi (A) Applications and Materials Science* 2015; 212: 2822–2829.
- [19] Veerapandiyar V, Benes F, Gindl T, et al. Strategies to improve the energy storage properties of perovskite lead-free relaxor ferroelectrics: A review. *Materials* 2020; 13: 1–47.
- [20] Zhang X, Deng X, Ren Y. Low temperature sintering and nonlinear dielectric properties of Li<sub>2</sub>O doped Ba<sub>0.6</sub>Sr<sub>0.4</sub>TiO<sub>3</sub> ceramics derived from the citrate method. *IOP Conference Series: Materials Science and Engineering* 2017; 207: 0–5.
- [21] Ma R, Cui B, Hu D, et al. Improving the dielectric properties of the Ba(Zr<sub>0.1</sub>Ti<sub>0.9</sub>)O<sub>3</sub>-based ceramics by adding a Li<sub>2</sub>O–SiO<sub>2</sub> sintering agent step by step. *International Journal of Nanoscience and Nanotechnology* 2020; 16: 233–241.
- [22] Amorós JL, Blasco E, Moreno A, et al. Effect of particle size distribution on the sinter-crystallisation kinetics of a SiO<sub>2</sub>–Al<sub>2</sub>O<sub>3</sub>–CaO–MgO–SrO glass-ceramic glaze. *Journal of Non-Crystalline Solids* 2020; 542: 120148.
- [23] Yang L. Effect of particle size on oxygen content and porosity of sintered Ti-6Al-4V. MSc Thesis, University of Utah, USA, 2015.
- [24] Nedelcu L, Ioachim A, Toacsan M, et al. Synthesis and dielectric characterization of Ba<sub>0.6</sub>Sr<sub>0.4</sub>TiO<sub>3</sub> ferroelectric ceramics doi: *Thin Solid Films* 2011; 519: 5811–5815.
- [25] Berent K, Komarek S, Lach R, et al. The effect of calcination temperature on the structure and performance of nanocrystalline mayenite powders. *Materials* 2019; 12(21): 3476.
- [26] Gatea HA. Impact of sintering temperature on crystallite size and optical properties of SnO<sub>2</sub> nanoparticles. *Journal of Physics: Conference Series* 2021; 1829: 012030.
- [27] Hu J. Grain Growth by Ordered Coalescence of Nanocrystals in Ceramics. PhD Thesis, Stockholm University, Sweden, 2013.
- [28] Kwon Y Bin, Kang JH, Han CS, et al. The effect of particle size and surface roughness of spray-dried bosentan microparticles on aerodynamic performance for dry powder inhalation. *Pharmaceutics* 2020; 12: 1–15.
- [29] Ulfa U, Kusumandari K, Iriani Y. The effect of temperature and holding time sintering process on microstructure and dielectric properties of barium titanate by co-precipitation method. *AIP Conference Proceedings* 2019; 2202: 020036.
- [30] Zeng L, Sun H, Peng T, et al. The sintering kinetics and properties of sintered glass-ceramics from coal fly ash of different particle size. *Results in Physics* 2019; 15: 102774.
- [31] Sandi D, Supriyanto A, Anif, et al. The effects of sintering temperature on dielectric constant of Barium Titanate (BaTiO<sub>3</sub>). *IOP Conference Series: Materials Science and Engineering* 2016; 107: 12069.
- [32] Fitriyana D, Suhaimi H, Sulardjaka S, et al. Synthesis of Na-P Zeolite from geothermal sludge. In: Murakami RI, Koinkar P, Fujii T, Kim TG., Abdullah H, editors. *NAC 2019: Proceedings of the 2nd International Conference on Nanomaterials and Advanced Composites*. Singapore: Springer, 2020, p 51-59.
- [33] Maharsi R, Jamaluddin A, Supriyanto A, et al. Crystalline characterization and dielectric constant of barium strontium titanates prepared by solid state reaction. *Advanced Materials Research* 2015; 1123: 123-126.
- [34] Kurnia, Heriansyah, Suharyadi E. Study on the influence of crystal structure and grain size on dielectric properties of manganese ferrite (MnFe<sub>2</sub>O<sub>4</sub>) nanoparticles. *IOP Conference Series: Materials Science and Engineering* 2017; 202: 012046.

# Effect of Sintering Temperature on the Physical Properties of Ba<sub>0.6</sub>Sr<sub>0.4</sub>TiO<sub>3</sub> Prepared by Solid-State Reaction

---

## ORIGINALITY REPORT

---

16%

SIMILARITY INDEX

11%

INTERNET SOURCES

12%

PUBLICATIONS

5%

STUDENT PAPERS

---

## MATCH ALL SOURCES (ONLY SELECTED SOURCE PRINTED)

---

1%

★ Min Wang, Xi Zuo, Kang Li, Genghua Cao. " Effects of Ba /Sr ratio on the microstructure, dielectric and ferroelectric properties of Ba Sr TiO films prepared by micro-arc oxidation ", Surface Engineering, 2021

Publication

---

Exclude quotes  On

Exclude matches  Off

Exclude bibliography  On